Yield design applied to a mechanically based non-local continuum

Ghada SAHLI [1], Oualid LIMAM [1]

[1]*Université de Tunis El Manar, Ecole Nationale d'Ingénieurs de Tunis, Laboratoire de Génie Civil, BP37, 1002 Tunis, Tunisia*

Abstract

Classical yield design theory provides upper and lower bounds of failure loads using local strength criteria. However, purely local formulations fail to reproduce size effects on failure loads of structures observed in quasi-brittle materials.

In this paper, a yield design formulation is developed for a mechanically based non-local continuum, in which long-range interactions between material points are introduced through central internal body forces. The formulation preserves classical Cauchy boundary conditions while enriching the internal power with a non-local contribution governed by an intrinsic length and a decay function. This work introduces a mechanically based non-local yield design approach that inherently accounts for size effects, offering a physically grounded extension of classical collapse analysis. Both kinematic (upper bound) and static (lower bound) approaches are established by defining local and non-local strength domains.

The exact solution is derived for a one-dimensional example with the same failure load derived by both approaches. This illustrates how the proposed framework leads to size-dependent axial strength.

An upper-bound non-local yield design approach of a cubic specimen under compression is used to predict a volume-dependent size effect of quasi-brittle materials with a Mohr–Coulomb local criterion and to interpret the *hourglass* failure mechanism.

Keywords

Yield design, Limit analysis, Failure load, Non-local continuum, Size effect

1. Introduction

Classical continuum mechanics describes internal interactions exclusively through Cauchy stresses acting on infinitesimal material surfaces. While this local framework is highly efficient for smooth deformation fields, it fails to reproduce experimentally observed size effects on stiffness and strength. These limitations have motivated the development of non-local continuum theories. Various non-local formulations have been proposed in the literature. Gradient-enhanced models and integral-type non-local models introduce additional kinematic or energetic contributions in order to account for material internal length scales [1].

Non-local approaches often raise difficulties in the mechanical interpretation of higher-order boundary conditions involving, for example, gradients of the strain field. Meanwhile, peridynamics models introduce a different concept, based on the interaction of material point pairs over distances, allowing internal forces to act non-locally rather than only at points of immediate contact [2].

A different and physically motivated class of models is provided by the mechanically based (MB) non-local continuum developed by Di Paola et al [3,4]. The key feature of this approach is the incorporation of non-local effects within a Cauchy continuum, represented by additional body forces acting on material points and associated by internal work to their relative displacements. The model is derived consistently from the principle of virtual power and preserves the classical Cauchy boundary conditions, which makes it particularly suitable for structures applications. In this respect, the MB approach shares conceptual similarities with peridynamics, while remaining fully compatible with standard continuum mechanics.

In parallel, yield design theory, as formalized by Salençon [5,6] provides a rigorous framework for collapse analysis based on lower bound and upper bound theorems. Yield design extends classical limit analysis by relying only on strength criteria and equilibrium or kinematic admissibility, without requiring an explicit rigid-plastic constitutive law. The notion of potentially supportable loads allows the analysis in a more general setting.

Despite significant advances in limit analysis and yield design for quasi-brittle materials, particularly in tension such as masonry [7,8,9], composite structures [10], and concrete microstructure [11], the question of size effect remains open. Previous attempts to incorporate scale effects in yield design have typically relied on strength criteria function of the area of the velocity jump surface, as proposed, for example, by Naija et al [11] for concrete microstructure failure. While these approaches are effective from a phenomenological standpoint, they call for further theoretical development to provide a more general foundation.

In this context, this work aims to advance the theoretical formulation of yield design for non-local continua. The MB model was chosen for its compatibility with classical boundary conditions in engineering applications. The framework naturally captures size effects through physically grounded long-range interactions, while maintaining the classical structure of yield design theory. Both approaches are developed in a general setting.

The objective of section 2 is to present kinematically admissible (**KA**) and statically admissible (**SA**) fields defined by the M.B model. Section 3 and 4 define respectively local and non-local failure criteria and correspondent elementary maximum internal power (support functions). Section 5 presents both upper and lower bound approaches for this model. Section 6 illustrates a rod under axial load with an exact solution given by both approaches with a size dependent failure load. Section 7 presents the upper bound approach applied to a cubic specimen under compression of a quasi-brittle material in tension with a Mohr-Coulomb local criterion. The objective is to highlight a volume size effect and to analyze failure mechanism. A discussing on the choice of the decay function is also presented.

2. Kinematic and static fields and principle of virtual power

Kinematic and static fields, as well as boundary conditions, are defined in accordance with those developed for nonlocal elasticity by Di Paola et al. [3,4] without relying on any constitutive laws.

Consider a body that is initially intact and free of cracks. Let Ω be an open bounded domain of $R^d (d = 1, 2 \; or \; 3)$, representing the reference configuration of this body. Its boundary $\partial\Omega$ is decomposed into two disjoint parts, $\partial\Omega_u$ and $\partial\Omega_t$, corresponding respectively to prescribed velocities and prescribed tractions.

The mechanical state of the body is described by the rate of displacement field (velocity field) $\mathbf{u}(\mathbf{x})$, defined as

$$\mathbf{u} : \Omega \rightarrow R^d$$

(1)

The velocity field is said to be **KA**, if it satisfies boundary conditions defined on components of $\mathbf{u}$ ($i \in \{1..d\}$) (Equation (2)).

$$u_i(\mathbf{x}) = 0 \quad for\ all\ \mathbf{x} \in \partial\Omega_u$$

(2)

The Cauchy stress tensor field is denoted by $\boldsymbol{\sigma}(\mathbf{x})$ and belongs to the space of symmetric second-order tensors (Equation (3)).

$$\boldsymbol{\sigma}(\mathbf{x}) \in S^d$$

(3)

The strain-rate tensor associated with the velocity field $\mathbf{u}$ is defined by Equation (4).

$$\boldsymbol{\varepsilon}(\mathbf{u}) = \frac{1}{2}(\, grad(\mathbf{u}) + \, grad(\mathbf{u})^T)$$

(4)

In addition to local stress interactions, long-range interactions are introduced through a pairwise interaction $\mathbf{q}(\mathbf{x},\boldsymbol{\xi})$, exerted by the material point $\boldsymbol{\xi}$ on the material point $\mathbf{x}$.

$$\mathbf{q} : \Omega \times \Omega \rightarrow R^d$$

(5)

The action–reaction principle is imposed in the form given by Equation (6).

$$\mathbf{q}(\mathbf{x}, \boldsymbol{\xi}) = -\mathbf{q}(\boldsymbol{\xi}, \mathbf{x})$$

(6)

The interaction force density expressed in ($N.m^{-2d}$) is decomposed using a scalar non-dimensional decay function g as follows:

$$\mathbf{q}(\mathbf{x}, \boldsymbol{\xi}) = g(|\mathbf{x} - \boldsymbol{\xi}|)\, \mathbf{q_0}(\mathbf{x}, \boldsymbol{\xi})$$

(7)

Where $\mathbf{q_0}(\mathbf{x}, \boldsymbol{\xi})$ is a vector defining the mechanical direction and intensity of the interaction. g should be chosen so that the integral $\int_\Omega \int_\Omega g(|\mathbf{x} - \boldsymbol{\xi}|)\, dV(\boldsymbol{\xi}) dV(\mathbf{x})$ decreases when measure V of Ω increases. In MB non-local elasticity [3,4], the decay function is usually positive and independent of the structural size, which leads to an apparent increase of this integral with size and consequently of the apparent stiffness. Here, to induce a decrease of the apparent strength as the domain size increases, the decay function is as a first hypothesis assumed to depend on the measure of Ω. A power-law

form (Equation 8) is adopted thereafter to simplify analytical developments, meanwhile, a discussion on its choice is presented in Section 7.

$$g(|\mathbf{x} - \boldsymbol{\xi}|) = \left(\frac{\wp^d}{V}\right)^{\alpha}, \quad \alpha > 0$$

(8)

The body is subjected to external loads, including a body force density $\mathbf{b}(\mathbf{x})$ and a prescribed traction $\mathbf{t}(\mathbf{x})$ on $\partial\Omega_t$, defined respectively by:

$$\mathbf{b} : \Omega \rightarrow R^d$$

$$\mathbf{t} : \partial\Omega_t \rightarrow R^d$$

(9)

With static boundary conditions

$$\boldsymbol{\sigma}(\mathbf{x}).\mathbf{n}(\mathbf{x}) = \mathbf{t}(\mathbf{x}) \quad on\ \partial\Omega_t$$

(10)

The mechanical problem is formulated through the principle of virtual power (Equation (11)), which states that, for any **KA** velocity field **u**,

$$P_{ext}(\mathbf{u}) = P_{int}(\mathbf{u})$$

(11)

The external power of external loads (given by Equation (9)), is defined as

$$P_{ext}(\mathbf{u}) = \int_{\Omega} \mathbf{b}(\mathbf{x}) \cdot \mathbf{u}(\mathbf{x}) dV + \int_{\partial\Omega_t} \mathbf{t}(\mathbf{x}) \cdot \mathbf{u}(\mathbf{x}) dS$$

(12)

The internal power is given by the sum of local and non-local contributions (Equation (13))[4].

$$P_{int}(\mathbf{u}) = \int_{\Omega} \boldsymbol{\sigma}(\mathbf{x}) : \boldsymbol{\varepsilon}(\mathbf{u}) dV + \frac{1}{2}\int_{\Omega}\int_{\Omega} \mathbf{q}(\mathbf{x}, \boldsymbol{\xi}) \cdot \big(\mathbf{u}(\boldsymbol{\xi}) - \mathbf{u}(\mathbf{x})\big) dV(\boldsymbol{\xi}) dV(\mathbf{x})$$

(13)

Applying principle (11) to any virtual velocity field and Ostrogradsky's theorem lead to the equilibrium Equation (14), using classical boundary condition (10).

$$div\ \boldsymbol{\sigma}(\mathbf{x}) + \int_{\Omega} \mathbf{q}(\mathbf{x}, \boldsymbol{\xi}) dV(\boldsymbol{\xi}) + \mathbf{b}(\mathbf{x}) = 0 \quad in\ \Omega$$

(14)

$\int_{\Omega} q(\mathbf{x}, \boldsymbol{\xi}) dV(\boldsymbol{\xi})$ is physically interpreted as the body force exerted on point **x** by all long-range interactions of the open domain Ω [3,4]. Figure 1 illustrates boundary conditions and external loads exerted on Ω if interpreted as a local continuum.

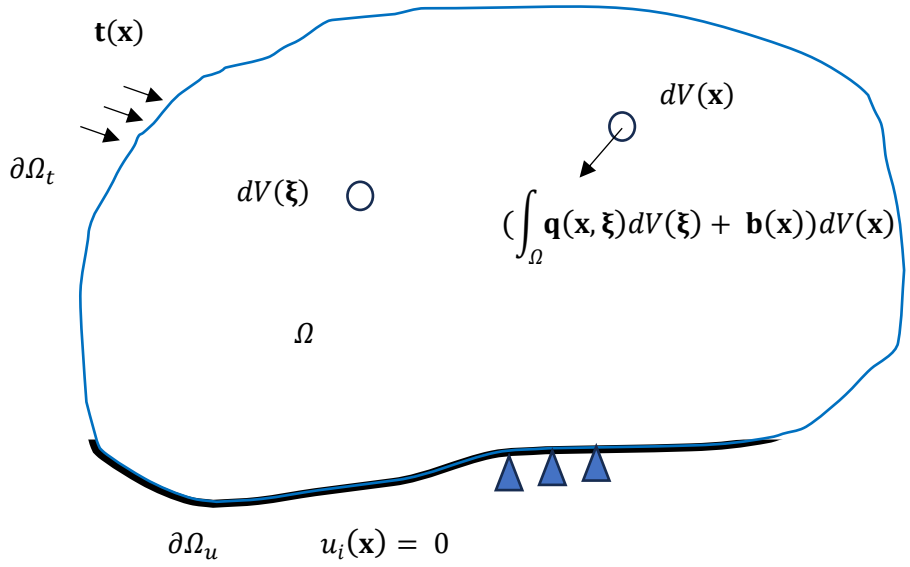

Figure 1. Boundary conditions and external load applied on the open domain Ω

Fields $\boldsymbol{\sigma}$ and $\mathbf{q}$ are said **SA**, if they verify equilibrium Equation (14), the action–reaction principle (Equation (6)) and static boundary condition (10).

3. Local strength criterion

The local material resistance is described by a convex strength domain

$$G_{loc} \subset S^d \tag{22}$$

defined in stress space.
For resistance, the Cauchy stress tensor must satisfy

$$\boldsymbol{\sigma}(\mathbf{x}) \in G_{loc} \;\; for\ all\ \mathbf{x} \in \Omega \tag{23}$$

The corresponding support function of the local criterion is defined by

$$\pi_{loc}(\boldsymbol{\varepsilon}) = \sup_{\sigma \in G_{loc}} (\boldsymbol{\sigma} : \boldsymbol{\varepsilon})$$

(24)

Which represents the maximum local resisting power density associated with the strain-rate tensor $\boldsymbol{\varepsilon}$.

4. Non-local strength criterion

Long-range interactions are described by the pairwise force density (Equation (7)). For any pair of material points $\mathbf{x}$ and $\boldsymbol{\xi}$, we define the colinear normal vector to the relative position vector as follows $\mathbf{n}(\mathbf{x},\boldsymbol{\xi})=\frac{\boldsymbol{\xi}-\mathbf{x}}{|\boldsymbol{\xi}-\mathbf{x}|}$. The mechanical interaction force $\mathbf{q_0}(\mathbf{x},\boldsymbol{\xi})$ is assumed to be collinear to the relative position (Equation (25)) and required to belong to a nonlocal convex strength domain (Equation (26)) where $q_0(x,\xi)$ is a scalar intensity of the non-local intensity.

$$\mathbf{q_0}(\mathbf{x},\boldsymbol{\xi}) = q_0(\mathbf{x},\boldsymbol{\xi})\,\mathbf{n}(\mathbf{x},\boldsymbol{\xi})$$

(25)

$$\mathbf{q_0}(\mathbf{x},\boldsymbol{\xi}) \in G_{ln} \quad \text{where} \quad G_{nl} \subset R^d$$

(26)

Because of convexity hypothesis and action-reaction principle, the non-local strength domain needs to be spherical which means that the scalar intensity of the interaction force is bounded in a form $-q_c' \le q_0(\mathbf{x},\boldsymbol{\xi}) \le q_c$. In the case of symmetric non local criterion, it becomes $|q_0(x,\xi)| \le q_c$. This simple symmetric non local criterion will be considered in a 1-D example of a rod presented in Section 6 in order to derive an exact bound of the failure load. In the case of a positive decay function and a symmetric non local criterion, the corresponding support function $\pi_{nl}(\mathbf{u}(\xi)-\mathbf{u}(x)) = \sup_{q_0(x,\xi)\in G_{nl}} \left(\mathbf{q}(\mathbf{x},\boldsymbol{\xi})\cdot\left(\mathbf{u}(\boldsymbol{\xi})-\mathbf{u}(\mathbf{x})\right)\right)$ is given by Equation (27).

$$\pi_{nl}\left(\mathbf{u}(\xi)-\mathbf{u}(x)\right) = g(|x-\xi|)q_c\left|\left(\mathbf{u}(\xi)-\mathbf{u}(x)\right).\frac{\boldsymbol{\xi}-\mathbf{x}}{|\boldsymbol{\xi}-\mathbf{x}|}\right|$$

(27)

Furthermore, to model failure of quasi-brittle materials in tension, where non local dissipation is driven by micro-cracking and mode I separation, we restrict the non-local strength domain G_{nl} to tension interaction only. Thus, the scalar intensity of the interaction force is bounded in a form $0 \le q_0(\mathbf{x},\boldsymbol{\xi}) \le q_c$. This non local criterion will be considered in the example of a cubic specimen under compression presented in section 7. In addition to this criterion and in the case of a positive decay function, in the corresponding support function $\pi_{nl}(\mathbf{u}(\boldsymbol{\xi})-\mathbf{u}(\mathbf{x})) = \sup_{q_0(\mathbf{x},\boldsymbol{\xi})\in G_{nl}} \left(q(\mathbf{x},\boldsymbol{\xi})\cdot\left(\mathbf{u}(\boldsymbol{\xi})-\mathbf{u}(\mathbf{x})\right)\right)$, the supremum is reached for $q_0(\mathbf{x},\boldsymbol{\xi}) = q_c$ only if relative displacement rate projected on interaction axis $\left(\mathbf{u}(\xi)-\mathbf{u}(x)\right).\frac{\boldsymbol{\xi}-\mathbf{x}}{|\boldsymbol{\xi}-\mathbf{x}|}$ is positive. Otherwise, the supremum is zero. This leads to a support function defined using by Equation (28). The term inside the brackets represents the relative extension

rate between any pair of material points projected on interaction axis and taking 0 when negative.

$$\pi_{nl}(\mathbf{u}(\xi)-\mathbf{u}(x)) = g(|x\ -\ \xi|)\ \mathrm{q}_c\ \langle\left(\mathbf{u}(\xi)-\mathbf{u}(x)\right).\frac{\boldsymbol{\xi}-\mathbf{x}}{|\boldsymbol{\xi}-\mathbf{x}|}\rangle_+$$

(28)

5. The upper and lower bound approaches of yield design

5.1. The upper bound approach

Within the framework of yield design theory, the collapse analysis is conducted using the kinematic (upper bound) approach [5,6]. This approach consists in comparing the power of the external loads to the maximum resisting internal power (Inequality (29)) to obtain an upper bound of the failure load for a given **KA** field **u**.

$$P_{ext}(\mathbf{u}) \leq\ P_{int}^{max}(\mathbf{u})$$

(29)

A general form of the maximum resisting internal power associated with a **KA** field involves a velocity discontinuity introduced through a velocity jump $[\mathbf{u}]$ across a surface Γ with a unit normal vector $\mathbf{n}'$, is given by Equation (30).

$$P_{int}^{\max}(\mathbf{u}) = \int_{\Omega}\pi_{loc}(\boldsymbol{\varepsilon})dV + \int_{\Gamma}\sup_{\sigma\in G_{loc}}(\boldsymbol{\sigma}\cdot\mathbf{n}'\cdot[\mathbf{u}])\,dS + \frac{1}{2}\int_{\Omega}\pi_{nl}(\mathbf{u}(\boldsymbol{\xi})-\mathbf{u}(\mathbf{x}))\,dV(\boldsymbol{\xi})dV(\mathbf{x})$$

(30)

5.2. The lower bound approach

Any external load, compatible with a **SA** local field $\boldsymbol{\sigma}$ and **SA** non-local field $\boldsymbol{q}$, and verifying local strength criterion (23) and non-local strength criterion (26), is a lower bound of the exact failure load.

6. One-dimensional illustrative example

We consider a one-dimensional rod occupying open interval $\Omega =]0, \mathrm{L}[$.

The rod is subjected to an axial load $\sum$ at $x = L$ with a kinematic boudary condition $\mathrm{u}(0) = 0$. A simple geometric decay function (Equation (31)) is introduced, depending on the characteristic material length ℓ and on the structural size L.

$$g(|x\ -\ \xi|) = \left(\frac{\ell}{L}\right)^{\alpha},\quad \alpha\ >\ 0$$

(31)

Strength domains are given by

$$G_{loc}\colon \sigma \leq\ f_t$$

$$G_{nl}\colon |q_0| \leq\ q_c$$

(32)

6.1. Kinematic (upper bound) approach

Two **KA** velocity fields are considered.

Case 1: Continuous velocity field

$$u(x) = \frac{u_0 x}{L}$$

(33)

The corresponding constant strain rate is

$$\frac{du}{dx} = \frac{u_0}{L}$$

(34)

The local maximal resisting power is

$$P_{loc}^{\max} = \int_0^L f_t \left|\frac{du}{dx}\right| dx = \mathrm{f_t u_0}$$

(35)

The non-local maximal resisting power is written as

$$P_{nl}^{\max} = \frac{1}{2}\int_0^L \int_0^L g(|x - \xi|) q_c |u(\xi) - u(x)| d\xi \, dx$$

(37)

Since

$$|u(\xi) - u(x)| = \left(\frac{u_0}{L}\right)|\xi - x|$$

$$P_{nl}^{max} = \left(\frac{q_c \mathrm{u_0}}{2L}\right)\left(\frac{\ell}{L}\right)^{\alpha} \int_0^L \int_0^L |\xi - x| d\xi \, dx$$

(38)

Using the identity, $\int_0^L \int_0^L |\xi - x| d\xi \, dx = \frac{L^3}{3}$, this leads to

$$P_{nl}^{max} = \frac{q_c \mathrm{u_0} L^2}{6}\left(\frac{\ell}{L}\right)^{\alpha}$$

(39)

An upper bound failure load Σ^+ follows from

$$P_{ext} = \sum^{+} \mathrm{u_0} = P_{loc}^{\max} + P_{nl}^{\max}$$

(40)

which gives

$$\Sigma^{+} = \left(f_t + \frac{q_c L^2}{6} \left(\frac{\ell}{L} \right)^{\alpha} \right)$$

(41)

Case 2: Discontinuous velocity field

A second **KA** field involves a velocity discontinuity at mid-span:

$$u(x) = 0 \quad for \quad 0 < x < \frac{L}{2}$$

$$u(x) = u_0 \quad for \quad L/2 < x < L$$

(42)

The velocity jump is

$$[u] = u_0$$

(43)

The local contribution reduces to the dissipation at the discontinuity:

$$P_{loc}^{\max} = f_t[u] = f_t u_0$$

(44)

Only pairs of points located on opposite sides of the discontinuity at $x = \frac{L}{2}$ contribute. The non-local resisting power is given by Equation (45).

$$P_{nl}^{max} = \left(\frac{q_c}{2} \right) \left(\frac{\ell}{L} \right)^{\alpha} \left(\int_{\{x < \frac{L}{2}\}} \int_{\{\xi > \frac{L}{2}\}} |u(\xi) - u(x)| d\xi \, dx + \int_{\{x > \frac{L}{2}\}} \int_{\{\xi < \frac{L}{2}\}} |u(\xi) - u(x)| d\xi \, dx \right)$$

(45)

Since $|u(\xi) - u(x)| = u_0$, one obtains

$$P_{nl}^{max} = \left(\frac{q_c u_0}{2} \right) \left(\frac{\ell}{L} \right)^{\alpha} 2 \left(\frac{L}{2} \right)^{2} = \frac{q_c u_0 L^2}{4} \left(\frac{\ell}{L} \right)^{\alpha}$$

(46)

Appling the upper bound approach, it gives an upper bound of the failure load associated with the discontinuous mechanism given by

$$\Sigma^{+} = \left(f_t + \frac{q_c L^2}{4} \left(\frac{\ell}{L} \right)^{\alpha} \right)$$

(47)

This value is higher than the one obtained with the continuous field (Equation (41)), showing that the continuous mechanism is more critical in the sense of the upper bound approach.

6.2. Static approach (lower bound)

The static equilibrium equation of the mechanically based non-local model Equation (14) becomes in one dimension:

$$\frac{d\sigma}{dx} + \int_0^L q(x,\xi)d\xi = 0$$

(48)

with boundary conditions

$$\sigma(0) = \sigma(\mathrm{L}) = \Sigma$$

(49)

The non-local interaction force must satisfy the action–reaction principle

$$q(x,\xi) = -q(\xi,x)$$

(50)

Case 1: Vanishing non-local interaction

We first consider the simple choice

$$q(x,\xi) = 0$$

(51)

The equilibrium equation reduces to

$$\frac{d\sigma}{dx} = 0$$

(52)

Hence, the stress field is constant and can be written as $\sigma(x) = C$. Choosing $C = f_t$, the local strength criterion (Equation (32)) is satisfied everywhere. Therefore, fields $\sigma(x) = f_t, q(x,\xi) = 0$ are statically admissible.

By the static (lower-bound) theorem of yield design, this stress field provides a lower bound of the collapse load

$$\Sigma^- = \mathrm{f_t}$$

(53)

Case 2: Non-local interaction

We now examine whether a non-zero non-local interaction may lead to a better lower bound. Consider the antisymmetric interaction force (Equation (54)) verifying $\mathrm{q}(\mathrm{x},\xi) = -q(\xi,\mathrm{x})$.

$q(x,\xi) = q_c\left(\frac{\ell}{L}\right)^{\alpha}\frac{1}{2}\sum_0^{+\infty}\left(\cos\left(\frac{(2n+1)\pi x}{L}\right)-\cos\left(\frac{(2n+1)\pi\xi}{L}\right)\right)$ for $x\ and\ \xi \in \left[\frac{L}{6},\frac{5L}{6}\right]$ and $q(x,\xi) = 0\ for\ x \in \left[0,\frac{L}{6}\right]\ or\ \left[\frac{5L}{6},L\right]$ and $\xi \in \left[0,\frac{L}{6}\right]\ or\ \left[\frac{5L}{6},L\right]$.

with $n \geq 0$ an integer.

(54)

The choice of interval $\left[\frac{L}{6},\frac{5L}{6}\right]$ comes from the fact that $\left|\sin\left(\frac{\pi x}{L}\right)\right| \geq \frac{1}{2}$ in this interval and the classical result:

$\sum_{n=0}^{N}\cos(2n+1)\frac{\pi x}{L} = \frac{\sin\left((2N+2)\frac{\pi x}{L}\right)}{2\sin\left(\frac{\pi x}{L}\right)}$ and $\left|\frac{\sin\left((2N+2)\frac{\pi x}{L}\right)}{2\sin\left(\frac{\pi x}{L}\right)}\right| \leq 1$ in this interval.

This choice satisfies also the action–reaction principle (50) and non-local strength criterion (32) because $|q_0| = q_c\left|\frac{1}{2}\sum_0^{+\infty}\left(\cos\left(\frac{(2n+1)\pi x}{L}\right)-\cos\left(\frac{(2n+1)\pi\xi}{L}\right)\right)\right| \leq q_c$ for $x\ and\ \xi \in \left[\frac{L}{6},\frac{5L}{6}\right]$.

Equilibrium Equation is given by

$$\frac{d\sigma}{dx} = -q_c\left(\frac{\ell}{L}\right)^{\alpha}\frac{1}{2}\int_{\frac{L}{6}}^{\frac{5L}{6}}\sum_0^{+\infty}\left(\cos\left(\frac{(2n+1)\pi x}{L}\right)-\cos\left(\frac{(2n+1)\pi\xi}{L}\right)\right)d\xi$$

(55)

Since $\int_{\frac{L}{6}}^{\frac{5L}{6}}\cos\left(\frac{(2n+1)\pi\xi}{L}\right)\ d\xi = 0$, the equilibrium Equation becomes

$$\frac{d\sigma}{dx} = -q_c\left(\frac{\ell}{L}\right)^{\alpha}\frac{L}{3}\sum_0^{+\infty}\cos\left(\frac{(2n+1)\pi x}{L}\right)$$

(56)

Integrating with respect to x gives

$$\sigma(x) = = -q_c\left(\frac{\ell}{L}\right)^{\alpha}\ \frac{L^2}{3\pi}\sum_0^{+\infty}\frac{\sin\left(\frac{(2n+1)\pi x}{L}\right)}{2n+1} + C$$

(57)

Where C is a constant. Fourier series $\sum_0^{+\infty}\frac{\sin\left(\frac{(2n+1)\pi x}{L}\right)}{2n+1}$, can be expressed also as $\frac{\pi}{4}f(x)$ as function of step function f defined by

$f(x) = 1$ if $0 < x < L$ and

$f(x) = -1\ if\ -L < x < 0$ or $L < x < 2L$.

This gives for $0 < x < L$

$$\sigma(x) = = -q_c \left(\frac{\ell}{L}\right)^{\alpha} \frac{L^2}{12} f(x) + C$$

If the integration constant C is chosen such that the local strength criterion (32) is exactly satisfied at the open domain $0 < x < L$, $C = f_t + q_c \left(\frac{\ell}{L}\right)^{\alpha} \frac{L^2}{12}$

$$\sigma(x) = f_t$$

(58)

At the boundary points x =0 and L, one obtains

$$\sigma(0) = \sigma(L) = f_t + \frac{q_c L^2}{6} \left(\frac{\ell}{L}\right)^{\alpha}$$

(59)

The failure load associated to a **S.A.** local and non-local static fields, with local and non-local strength criteria satisfied at $0 < x < L$ is given by Equation (60).

$$\Sigma^{-} = f_t + \frac{q_c L^2}{6} \left(\frac{\ell}{L}\right)^{\alpha}$$

(60)

As the same value was found by the upper bound approach Equation (41), it is concluded that the exact failure load in the frame of the model hypothesis is $f_t + \frac{q_c L^2}{6} \left(\frac{\ell}{L}\right)^{\alpha}$.

Furthermore, $\alpha > 2$ should be chosen to obtain a size effect on the failure load, namely a decrease of the failure load with increasing rod length, where f_t denotes the axial failure load as L tends to infinity.

7. A cubic solid under compression

7.1. Compressive strength derived by the upper bound approach applied

Consider a cubic solid defined by the open domain Ω defined by material points in a cartesian orthonormal system with coordinates $(x_1, x_2, x_3) \in \left]\frac{-L}{2}, \frac{L}{2}\right[\times \left]\frac{-L}{2}, \frac{L}{2}\right[\times]0, L[$. Consider a quasi-brittle material in tension, for an example with a Mohr-Coulomb local criterion and a non-local criterion in a form $0 \leq q_0(\mathbf{x}, \boldsymbol{\xi}) \leq q_c$, so that, Equation (28) is assumed for the associated support function. Cohesion and friction angle are denoted respectively by C and φ. An imposed velocity U is applied at the upper surface (x_3=L) of an area L^2 with an associted reaction denoted F such that $F = p\ L^2$ where p is the mean pressure applied. A three-dimensional velocity filed **u** is considered. This velocity field is **KA** if boundary conditions (61) are fulfilled, together with the constraint preventing rigid body motion.

$$u_3(x_1, x_2, 0) = 0$$

$$u_3(x_1, x_2, L) = -U$$

(61)

The power of the external forces is given by Equation (62)

$$P_e = p\ U\ L^2$$

(62)

A particular velocity field $\mathbf{u}$ is considered with a constant strain rate (Equation (63)). This was proposed by Salençon [5] as an optimal mechanism given the exact solution for the limit load when compared with the static lower bound approach within a local yield design approach. In the case of local yield design approach, it exists mechanisms with a velocity discontinuity which give also the exact failure load for this compression problem [5]. As it was shown in Section 6 for the non-local yield design of a rod under axial load that the mechanism with a velocity jump give a higher failure load, this motivates a choice of a continuous velocity field (Equation (63)).

$$u_3(x_1, x_2, x_3) = -U\frac{x_3}{L}$$

$$u_1(x_1, x_2, x_3) = U\ x_1\ \tan^2\left(\frac{\pi}{4} + \frac{\varphi}{2}\right)/(2L)$$

$$u_2(x_1, x_2, x_3) = U\ x_2\ \tan^2\left(\frac{\pi}{4} + \frac{\varphi}{2}\right)/(2L)$$

(63)

The local maximal internal power is given by Equation (64).

$$P_{loc}^{max} = 2CUL^2\tan\left(\frac{\pi}{4} + \frac{\varphi}{2}\right)$$

(64)

Non local maximum internal power is expressed using support function (28) for quasi-brittle materials in tension which leads to Equation (65).

$$P_{nl}^{max} = \frac{1}{2}\mathrm{q_c}\left(\frac{\ell}{L}\right)^{3\alpha}\int_{\Omega}\int_{\Omega}\langle\left(\mathbf{u}(\boldsymbol{\xi}) - \mathbf{u}(\mathbf{x})\right).\frac{\boldsymbol{\xi} - \mathbf{x}}{|\boldsymbol{\xi} - \mathbf{x}|}\rangle_+\, dV(\boldsymbol{\xi})dV(\mathbf{x})$$

(65)

Where $(\mathbf{u}(\xi) - \mathbf{u}(\mathbf{x})).\frac{\boldsymbol{\xi}-\mathbf{x}}{|\boldsymbol{\xi}-\mathbf{x}|} = \frac{U}{L|\boldsymbol{\xi}-\mathbf{x}|}\left(\frac{T}{2}(\xi_1 - \mathrm{x}_1)^2 + \frac{\mathrm{T}}{2}(\xi_2 - \mathrm{x}_2)^2 - (\xi_3 - \mathrm{x}_3)^2\right)$ and where T=$\tan^2\left(\frac{\pi}{4} + \frac{\varphi}{2}\right)$.

Or also

$$P_{nl}^{max} = \frac{1}{2}\mathrm{q_c}\left(\frac{\ell}{L}\right)^{3\alpha}\frac{U}{L}\int_{-L/2}^{L/2}\int_{-L/2}^{L/2}\int_{-L/2}^{L/2}\int_{-L/2}^{L/2}\int_0^L\int_0^L \langle\frac{\left(\frac{\mathrm{T}}{2}(\xi_1 - \mathrm{x}_1)^2 + \frac{\mathrm{T}}{2}(\xi_2 - \mathrm{x}_2)^2 - (\xi_3 - \mathrm{x}_3)^2\right)}{\sqrt{(\xi_1 - \mathrm{x}_1)^2 + (\xi_2 - \mathrm{x}_2)^2 + (\xi_3 - \mathrm{x}_3)^2}}\rangle_+ d\xi_1\, d\xi_2\, d\xi_3 dx_1\, dx_2 dx_3$$

And this the non-local dissipation can be expressed by Equation (66).

$$P_{nl}^{max} = \frac{1}{2}\mathrm{q_c}\left(\frac{\ell}{L}\right)^{3\alpha} UL^4\, I(T)$$

(66)

Where the integral denoted $I(T)$ can be expressed in non-dimensional form using a specific change of variables (Equation (67)).

$$I(T) = \int_{-1/2}^{1/2}\int_{-1/2}^{1/2}\int_{-1/2}^{1/2}\int_{-1/2}^{1/2}\int_{0}^{1}\int_{0}^{1} \left\langle \frac{\left(\frac{T}{2}(\hat{\xi}_1-\hat{x}_1)^2+\frac{T}{2}(\hat{\xi}_2-\hat{x}_2)^2-(\hat{\xi}_3-\hat{x}_3)^2\right)}{\sqrt{(\hat{\xi}_1-\hat{x}_1)^2+(\hat{\xi}_2-\hat{x}_2)^2+(\hat{\xi}_3-\hat{x}_3)^2}} \right\rangle_+ d\hat{\xi}_1\, d\hat{\xi}_2\, d\hat{\xi}_3\, d\hat{x}_1\, d\hat{x}_2\, d\hat{x}_3$$

(67)

Equating external power (62) and sum of local and non-local maximal internal powers an upper bound of the compressive strength is derived and given by Equation (68).

$$\mathbf{p}^+ = 2C\tan\left(\frac{\pi}{4}+\frac{\varphi}{2}\right) + \frac{1}{2}\mathrm{q_c}\left(\frac{\ell}{L}\right)^{3\alpha} L^2\, I(T)$$

(68)

7.2. Physical interpretation

The purely geometric integral $I(T)$ depends solely on the relative distances between material points. Because it depends strictly on coordinate differences, its overall value is invariant under any spatial translation of the reference frame within the cubical domain. Furthermore, the use of Macaulay brackets inherently restricts the non-local dissipation to a specific active zone. Non local energy dissipation occurs exclusively for pairs of material points $\mathbf{x}$ and $\boldsymbol{\xi}$, where the relative position vector $\boldsymbol{\xi}-\mathbf{x}$ is outside a vectorial vertical cone governed by the condition (69).

$$\frac{\mathrm{T}}{2}((\xi_1-\mathrm{x}_1)^2+(\xi_2-\mathrm{x}_2)^2) > (\xi_3-\mathrm{x}_3)^2$$

(69)

This means that the vectorial zone where non local dissipation occurs is defined by Equation (70) where θ is the angle of vector $\boldsymbol{\xi}-\mathbf{x}$ with respect to the vertical axis which means that $\theta > \theta_c$ with $\theta_c = Atan(\sqrt{\frac{2}{T}})$ (figure2).

$$\tan(\theta) = \frac{\sqrt{((\xi_1-\mathrm{x}_1)^2+(\xi_2-\mathrm{x}_2)^2)}}{|\xi_3-\mathrm{x}_3|} > \sqrt{\frac{2}{T}}$$

(70)

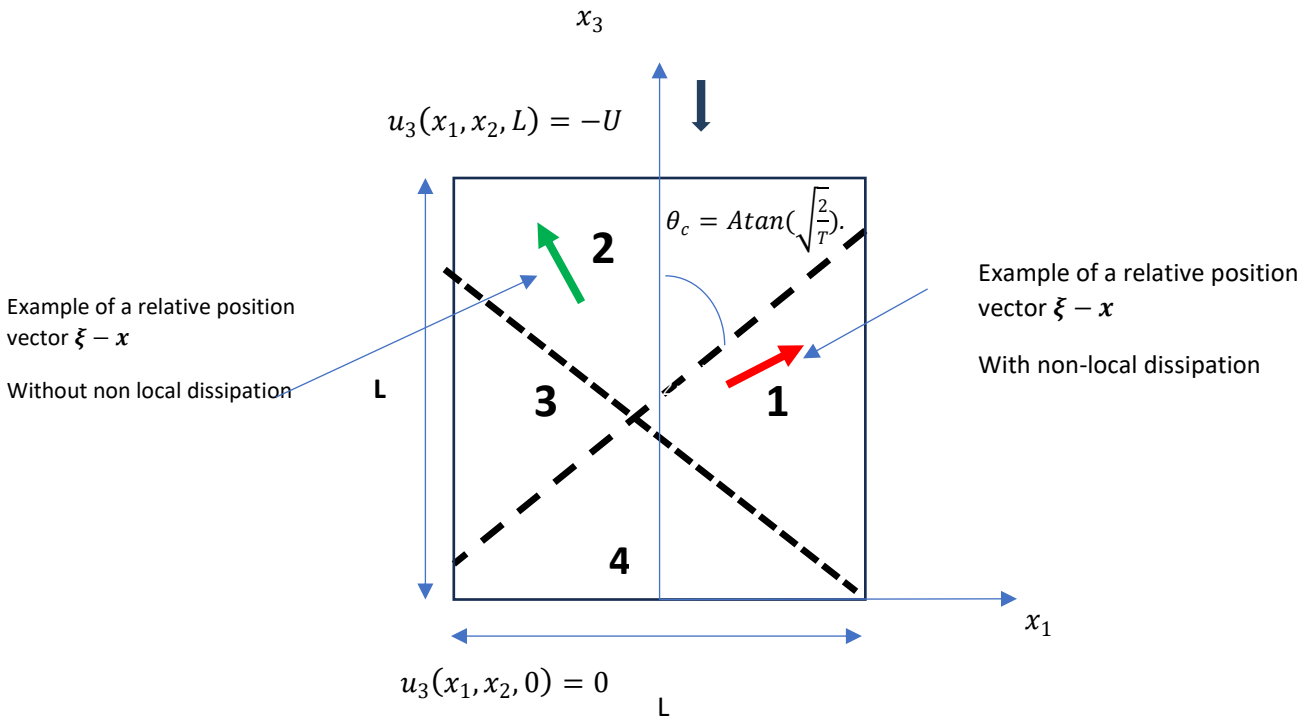

Figure 2. *Hourglass mechanism* and non-local dissipation directions of the relative position vector

This induces greater dissipation (both local and non-local), particularly in directions near the horizontal plane, which explains why failure initiates along these orientations. This provides a physical interpretation of the failure mechanism experimentally observed in concrete specimens under compression, commonly referred to as the hourglass mechanism [12].

It should be noted that, within this non-local approach, this phenomenon has been explained using a continuous field description. Experimental tests conducted on cubic concrete specimens by Yankelevsky [12] show that vertical cracking or inclined shear bands appear first. Upon reaching ultimate failure and removing the loose concrete debris, the intact core of the specimen is exposed, revealing an hourglass shape. In our approach, the formation of vertical cracks is consistent with the continuous field and its associated local dissipation through lateral extension, whereas the development of shear bands is captured by the non-local dissipation.

Furthermore, by applying the derived strength (Equation 68), for example to compression tests on concrete with an order of $(-3\alpha + 2 \approx -0.15)$, $(\alpha \approx 0.7)$ size effect law is obtained that is consistent with certain experimental size effect power laws for high-strength concrete [11].The strength decreases as a function of specimen size according to a power law with an exponent of k=-0.15, reaching an asymptote $2C\tan\left(\frac{\pi}{4} + \frac{\varphi}{2}\right)$ as the dimension tends toward infinity. Similarly, this size-dependent behavior is observed in other Mohr-Coulomb materials; Experimental studies show that compressive strength of rock decreases with the increase of rock size fitting result shows k varies from 0.08 to 0.77 [13].

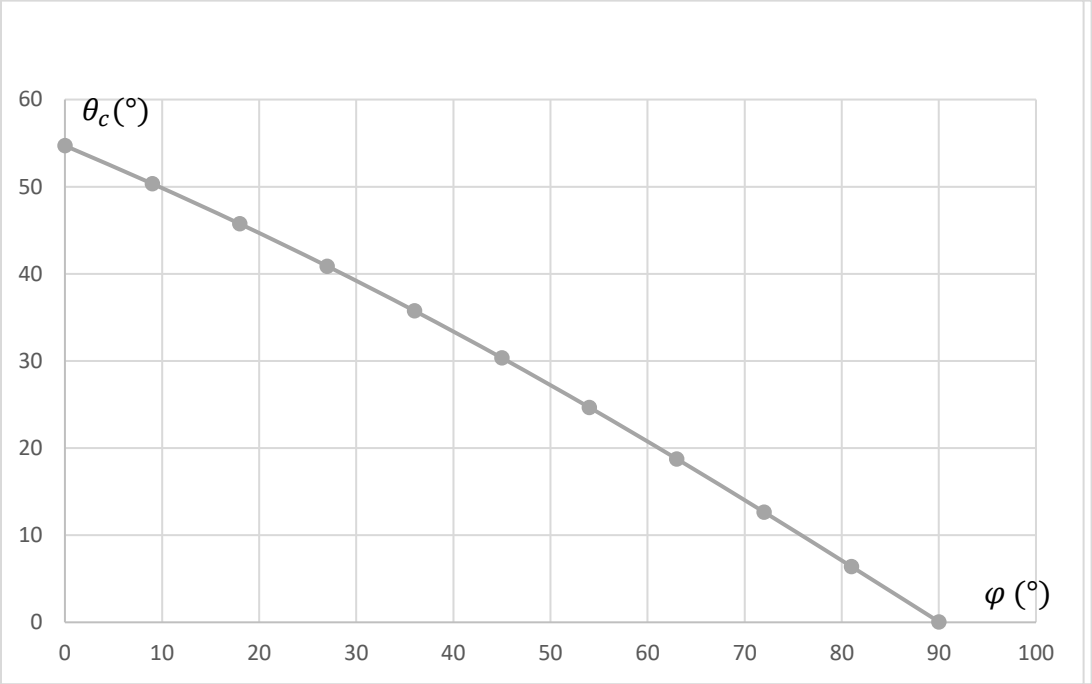

Figure 3. Critical angle $\theta_c = Atan(\sqrt{\frac{2}{T}})$ as function of friction angle φ

It is important to emphasize the role of the local failure criterion, namely the Mohr–Coulomb criterion, in the resulting size effect. Within the present nonlocal framework, the critical angle θ_c reaches its maximum in the limiting case $\varphi = 0$, which corresponds to a purely cohesive behavior equivalent to the Tresca criterion (Figures 2 and 3). In this case, $I(T)$ is minimal and the nonlocal dissipation contribution is therefore also minimal. For concrete and rocks, the critical parameter θ_c is low, which in turn leads to a higher nonlocal dissipation term. This trend is consistent with the size-effect power law proposed by Zhao et al. [13] for the compressive strength of rocks.

7.3. Discussion on decay function

As a perspective for future research, the development of a numerical solution would require a kernel g independent of L, modeled as a partially negative "Mexican hat" function. In this case, the interaction is strongest and most visible between two material points in close proximity, within a radius defined by the characteristic length ℓ. This approach allows for the construction of families of kinematically admissible numerical fields, where the solution is derived through a minimization problem. The partially negative nature of g is essential here in order to ensure a reduction in the limit load when an increasing homothety is applied to the structure, thereby predicting the scaling behavior of concrete specimens.

8. Conclusion

A yield design framework for mechanically based non-local continua has been proposed, combining classical Cauchy mechanics with long-range interactions. Both kinematic and static approaches were formulated using local and non-local strength criteria, without assuming constitutive laws.

The application of this framework to the 1D problem demonstrated that the upper bound, derived through the kinematic approach, is equal to the lower bound obtained through the static approach, thereby providing the exact yield load. A key finding within the kinematic approach is that the optimal collapse mechanism is continuous. Interestingly, a mechanism involving a velocity discontinuity (a jump in the velocity field) gives a strictly higher value than the continuous one. For this problem, this stands in contrast with the case of a local yield design approach applied to this problem where both mechanisms lead to the same failure load.

While the kinematic approach proved efficient, the static approach remains analytically fastidious and difficult to implement for complex geometries. This difficulty motivated the application of the kinematic approach to a 3D cubic specimen under compression using a continuous velocity field.

While initial one-dimensional applications highlighted the fundamental emergence of size effects, the extension to a three-dimensional uniaxial compression test demonstrated the physical relevance of the model. Assuming a Mohr-Coulomb local criterion, the kinematic approach naturally restricts the active yielding volume based on the relative displacement of material points. The model theoretically predicts the existence of a non-dissipative vectorial zone ($\theta > \theta_c$) governed by the internal friction angle. This analytically kinematic field mirrors the classic "hourglass" or shear cone failure modes observed in concrete compression testing. This theoretical outcome is highly consistent with established size effect laws for quasi-brittle materials.

This approach offers a consistent, physically grounded extension of classical yield design, enabling evaluation of size-dependent failure loads in quasi-brittle materials. Extensions to more complex problems require a non-geometrically dependent decay functions and numerical solutions which may enhance its applicability to structures.

The kinematic approach is particularly relevant from an engineering perspective, since the optimal kinematic fields are inspired by real observations.

References

[1] Bažant, Z.P., Jirásek, M., 2002. Nonlocal integral formulations of plasticity and damage: survey of progress. *Journal of Engineering Mechanics*, 128(11), 1119–1149.

[2] Silling, S.A., 2000. Reformulation of elasticity theory for discontinuities and long-range forces. *Journal of the Mechanics and Physics of Solids*, 48(1), 175–209. *(Note : volume et pages ajoutés)*

[3] Di Paola, M., Failla, G., Zingales, M., 2010. Mechanically based non-local elasticity: variational principles. *International Journal of Solids and Structures* 47 (2010) 539–548

10.1016/j.ijsolstr.2009.09.029

[4] Di Paola M, Failla G, Pirrotta A, Sofi A, Zingales M. 2013 The mechanically based non-local elasticity: an overview of mainresults and future challenges. Phil Trans RSocA371:20120433. http://dx.doi.org/10.1098/rsta.2012.0433

[5] Salençon, J., 1983. *Calcul à la rupture et analyse limite*. Presses de l'École Nationale des Ponts et Chaussées, Paris.

[6] Salençon, J., 2013. *Yield Design*. ISTE Ltd and John Wiley & Sons, Inc doi 10.1002/9781118648988

[7] Milani, G., Bucchi, A., 2010. Kinematic FE homogenized limit analysis model for masonry curved structures strengthened by near surface mounted FRP bars. *Composite Structures*, 93(1), 239–258.

[8] Sahli, G., Limam, O., 2025. Macroscopic strength criteria for bio-inspired interlocking masonry: A yield design approach. *Engineering Failure Analysis*, 182(Part B), 110071.

[9] De Buhan, P., De Felice, G., 1997. A homogenization approach to the ultimate strength of brick masonry. *Journal of the Mechanics and Physics of Solids*, Volume 45, Issue 7, Pages 1085-1104

https://doi.org/10.1016/S0022-5096(97)00002-1.

[10] Limam, O., Foret, G., Ehrlacher, A., 2003. RC two-way slabs strengthened with CFRP strips: experimental study and a limit analysis approach. *Composite Structures*, 60(4), 467–471.

[11] Naija, A., Hassen, G., Limam, O., Miled, K., 2020. Numerical study of the biaxial compressive strength of high strength concrete based on a yield design micromechanical approach. *International Journal for Numerical and Analytical Methods in Geomechanics*, 44(6), 772–781.

[12] Yankelevsky D.Z., 2024. The uniaxial compressive strength of concrete: revisited, Materials and Structures 57:144

[13] Zhao Y. , Mishra B., Shi Q., Zhao G., 2023. Size-dependent Mohr–Coulomb failure criterion, Bulletin of Engineering Geology and the Environment 82:218

https://doi.org/10.1007/s10064-023-03243-y

During the preparation of this work the authors used [Gemini] in order to [revise English]. After using this tool/service, the authors reviewed and edited the content as needed and takes full responsibility for the content of the published article.